ASIAN JOURNAL OF CIVIL ENGINEERING (BHRC) VOL. 14, NO. 6 (2013)
PAGES 859-879

NONLINEAR SEISMIC RESPONSE OF A CONCRETE ARCH DAM TO SPATIALLY VARYING EARTHQUAKE GROUND MOTIONS

H. Mirzabozorg*[1], M. Akbari[1] and M.A. Hariri-Ardebili[2]
[1]Department of Civil Engineering, KN. Toosi University of Technology, Tehran, Iran.
[2]Department of Civil, Environmental and Architectural Engineering, University of Colorado at Boulder, Boulder, USA.

Received: 10 February 2013; **Accepted:** 20 March 2013

ABSTRACT

Spatially uniform ground motion is an assumption that is often made for structural analyses of arch dams. However, it has been recognized for many years that the ground motion is non-uniform due to large distances between the supports of structures such as bridges and dams. In this paper, a comprehensive investigation on the seismic response of dam-reservoir-foundation systems subjected to spatially varying ground motions is represented. Monte Carlo simulation approach is utilized for generating spatially non-uniform ground motions. A high arch dam is selected as numerical example to investigate nonlinear seismic behaviour of the coupled system. Reservoir is modelled as compressible material and the foundation is supposed to be mass-less medium. Seismic responses of the dam due to incoherency and wave passage are investigated. According to the results, the non-uniform input produces a response that is substantially different from the response produced with uniform input and can increases the structural response of the system.

Keywords: Concrete arch dam; incoherency; non-uniform excitation; wave passage.

1. INTRODUCTION

Structures that have extended supports such as pipelines, tunnels, bridges and dams, are subjected to the effect of spatially variable ground motions during an earthquake. When earthquake waves travel through the ground which supports the long-span structures, both amplitude and frequency content change continually. In this condition waves arrive to various points of the structure with time lag and different frequency contents. Variations in

* E-mail address of the corresponding author: mirzabozorg@kntu.ac.ir (H. Mirzabozorg)

the ground motion characteristics arise mainly from three sources; the "wave passage effect" due to the differences in the arrival time of waves at supporting points depending on their relative distances away from the source; the "incoherency effect" due to reflections and refractions of seismic waves through the soil during propagation that causes changing in amplitude and frequency away from their source; and finally, the "site-response effect" due to the differences in local soil conditions at the supporting points [1, 2]. So, in wave passage based models, two separate support points of the considered structure undergo exactly the same motion (in amplitude and frequency) but with a time shift while in incoherency based models, the two support points undergo modified (in amplitude and frequency) versions of the same ground motion.

Many researchers have investigated the response of long span structures to differential (asynchronous) support excitations. Most of them have used relatively simple models to describe the structure. Effect of asynchronous and multiple supports input in analysis of beams and bridges have been considered by many researchers. Dams are important engineering structures which can cause catastrophic hazards when earthquakes happen. So design of a dam is a worthy attention issue in the countries with high seismicity. A lot of works in the field of seismic analysis of arch dams has been done. Listen However, few works have investigated effects of asynchronous on the seismic behavior of concrete dams. Chen and Harichandran [3] conducted the sensitivity analysis of the random vibration response of Santa Felicia earth dam. They found that the pseudo-static effect would not be diminished and various coherency models lead to variability in the peak responses. Baraktar et al. [4, 5] analyzed the effect of wave propagation on the response of Sariyar concrete gravity dam. They reported that horizontal, vertical and shear stresses in the foundation generally increase with decreasing propagation velocity and at a cross section close to the base of the dam, horizontal stresses increase with decreasing velocity but vertical and shear stresses don't exhibit a certain pattern. Meso et al. [6] analyzed an arch dam subjected to incident body (P-, SV- and SH-) and surface (Rayleigh) waves. They concluded that local topography causes scattering of the incident waves and results a ground motion pattern which is different from what would have resulted in the half-space. Nowak and Hall [7] analyzed the seismic response of Pacoima dam in two parts. Their work showed that the stresses for a full reservoir are higher than the stresses for an empty one and non-uniformity in the stream component of the excitation tends to decrease the response. Alves and Hall [8, 9] analyzed the effect of spatially variable excitations on the nonlinear response of Pacoima dam using available seismic data in the dam site. Results showed that for uniform excitations stresses and joints opening are largest in the center part of the dam away from the abutments and also, cracks formed mostly in the central part. On the other hand, a significant portion of the response due to spatially variable excitations is due to pseudo-static component. The stresses along the abutments and in the center of the downstream face of the dam are dominated by the pseudo-static response, whereas those near the central parts in vicinity of the crest are due to dynamic contribution. Therefore, joints opening can be observed along the abutments caused by the pseudo-static effects.

Stochastic and deterministic dynamic responses of gravity dam-reservoir systems were compared using the displacement fluid finite elements by Bayraktar et al. [10]. It was generally observed that the displacements, stresses and hydrodynamic pressures obtained

from the stochastic dynamic analysis of gravity dam-reservoir systems are much smaller than those of the deterministic dynamic analysis. Mirzabozorg et al. [11] investigated the effects of non-uniform excitation due to spatially variation of seismic waves under the reservoir bottom on linear and nonlinear responses of arch dams. It was observed that the non-uniform excitation decreases the crest displacements in the stream directions in comparison with uniform excitation. Nonlinear Response of Earthfill dams to spatially varying ground motion which includes the wave passage, incoherence and site response effects was investigated by Haciefendioglu and Soyluk [12]. Chopra and Wang [13] computed the response of two arch dams to spatially varying ground motions recorded during earthquake by developed linear analysis procedure, which includes dam-water-foundation rock interactions effects. They concluded that the influence of spatially varying ground motion for the same dam could differ from one earthquake to the next, depending on the epicenter location and the focal depth of the earthquake relative to the dam site. In the other research Wang and Chopra [14] used the available substructure method and computer program for earthquake response analysis of arch dams, including the effects of dam-water-foundation rock interaction to consider spatial variations in ground motions around the canyon. Mirzabozorg et al. [15] Investigated the wave passage and incoherency effects seperatly in seismic response of an arch dam. They found that the coherency effect overshadows the wave passage effect and the results obtained from non-uniform excitation of the coupled dam-reservoir-foundation system, including the wave passage effect, is close to the results of the model when it is uniformly excited.

In the current study, Monte-Carlo simulation approach was utilized for generating spatially non-uniform ground motions. Double curvature Dez dam was selected for numerical example and all contraction and perimetral joints were modeled based on as-built drawings to investigate travelling wave and incoherency effects. Reservoir was modeled as compressible material based on Eulerian approach and foundation was assumed to be massless.

2. SPATIALLY VARIATION IN GROUND MOTION

The spatial variation of ground motion records can be attributed to the following three mechanisms [16]:

- The difference in arrival times of the seismic waves at different locations, commonly known as the “wave passage effect”;
- The change in shape of the propagating waveform due to multiple scatterings of the seismic waves in the highly inhomogeneous soil medium, referred to as the “incoherence effect”; and
- The change in amplitude and frequency content of ground motion at different locations on the ground surface due to different local soil conditions known as the “local site effect”.

In this paper, an iterative algorithm shown in Fig. 1 proposed by Saxena [17] and Deodatis [18] is used to generate differential acceleration time histories at several prescribed locations on the ground surface that are compatible with prescribed response spectra. The methodology is described as follows by considering that the acceleration time histories at a

specified number of locations on the ground surface constitute a multi-variate, non-stationary stochastic process (non-stationary stochastic vector process) [19]. To be specific, consider a *n*-variate non-stationary stochastic vector process with components $f_j^0(t)$; $j=1,2,...,n$ having mean value equal to zero; i.e. $\varepsilon\left[f_j^0(t)\right]=0$, $j=1,2,...,n$.

Different target acceleration response spectrum $RSA_i(\omega)$; $i=1,2,...,n$ can be assigned to each of these points, since those points can generally be on different local soil conditions. Complex coherence functions $\Gamma_{jk}(\omega)$; $j,k=1,2,\ldots,n$; $j\neq k$ are prescribed between pairs of points and modulating functions $A_j(t)$; $j=1,2,...,n$ are assigned at each point.

Complex coherence functions are given by:

$$\Gamma_{jk}(\omega)=\gamma_{jk}(\omega)\exp\left[-i\frac{\omega\xi_{jk}}{\upsilon}\right];\quad j,k=1,2,...,n;\quad j\neq k \tag{1}$$

where, $\gamma_{jk}(\omega)$; $j,k=1,2,...,n$; $j\neq k$ are the (stationary) coherence functions between points *j* and *k*; $\exp\left[-i\frac{\omega\xi_{jk}}{\upsilon}\right]$ is the wave propagation term where $\xi_{jk}(\omega)$ is the distance between points j and k and υ is the velocity of wave propagation.

The power spectral density functions $S_j(\omega)$, $j=1,2,\ldots,n$ in the first iteration are initialized to a constant (non-zero) value over the entire frequency range.

$$S^0(\omega,t)=\begin{bmatrix} S_1(\omega) & \sqrt{S_1(\omega)S_2(\omega)}\Gamma_{12}(\omega) & \cdots & \sqrt{S_1(\omega)S_n(\omega)}\Gamma_{1n}(\omega) \\ \sqrt{S_2(\omega)S_1(\omega)}\Gamma_{21}(\omega) & S_2(\omega) & \cdots & \sqrt{S_2(\omega)S_n(\omega)}\Gamma_{2n}(\omega) \\ \vdots & \vdots & \ddots & \vdots \\ \sqrt{S_n(\omega)S_1(\omega)}\Gamma_{n1}(\omega) & \sqrt{S_n(\omega)S_2(\omega)}\Gamma_{n2}(\omega) & \cdots & S_n(\omega,t) \end{bmatrix}_{n\times n} \tag{2}$$

For the purpose of this study, a special case of Eq. (2) is assumed to hold:

$$S_{jj}^0(\omega,t)=|A_j(\omega,t)|^2\,S_j(\omega)\ ;\ j=1,2,\ldots,n \tag{3}$$

$$S_{jk}^0(\omega,t)=A_j(\omega,t)A_k(\omega,t)\sqrt{S_j(\omega)S_k(\omega)}\Gamma_{jk}(\omega)\ ;\ j,k=1,2,\ldots,n\ ,\quad j\neq k \tag{4}$$

In order to simulate samples of the *n*-variate non-stationary stochastic process $f_j^0(t)$; $j=1,2,...,n$, (stationary) cross-spectral density matrix $S^0(\omega)$ given in Eq. (2) is factorized into the following product:

$$S_f^0(\omega,t)=H(\omega,t)H^{T*}(\omega,t) \tag{5}$$

$$H(\omega,t)=\begin{bmatrix} H_{11}^{0}(\omega,t) & & & \\ H_{21}^{0}(\omega,t) & H_{22}^{0}(\omega,t) & & \\ \vdots & \vdots & \ddots & \\ H_{n1}^{0}(\omega,t) & H_{n2}^{0}(\omega,t) & \cdots & H_{nn}^{0}(\omega,t) \end{bmatrix} \tag{6}$$

Using Cholesky's decomposition method, the diagonal elements of $H(\omega)$ are real and non-negative functions of ω while the off-diagonal elements are generally complex functions of ω. The elements of $H(\omega)$ can be written in polar form as:

$$H_{jk}(\omega)=\left|H_{jk}(\omega)\right|e^{i\theta_{jk}(\omega)}, \quad j>k \tag{7}$$

where;

$$\theta_{jk}(\omega)=\tan^{-1}\left(\frac{\mathrm{Im}\left[H_{jk}(\omega)\right]}{\mathrm{Re}\left[H_{jk}(\omega)\right]}\right) \tag{8}$$

After setting up the cross-spectral density matrix given in Eq. (2) according to a prescribed coherence function and a velocity of wave propagation, the stationary ground motion time histories are generated using the simulation formula given in Eq. (9).

$$g_j(t)=2\sum_{m=1}^{n}\sum_{l=1}^{N}\left|H_{jm}(\omega_l)\right|\sqrt{\Delta\omega}\cos\left[\omega_l t-\theta_{jm}(\omega_l)+\phi_{ml}\right], \quad j=1,2,...,n \tag{9}$$

where;

$$\omega_l=l\Delta\omega, \quad l=1,2,...,N \tag{10}$$

$$\Delta\omega=\frac{\omega_u}{N} \tag{11}$$

$$\theta_{jm}(\omega_l)=\tan^{-1}\left(\frac{\mathrm{Im}\left[H_{jm}(\omega_l)\right]}{\mathrm{Re}\left[H_{jm}(\omega_l)\right]}\right) \tag{12}$$

The quantities $\{\phi_{ml}\}; m=1,2,...,n; l=1,2,...,N$ appearing in Eq. (9) are n sequences of independent random phase angles distributed uniformly over the interval $[0,2\pi]$. In Eq. (11), ω_u represents an upper cut-off frequency beyond which the elements of the cross-

spectral density matrix in Eq. (2) maybe assumed to be zero for anytime instant *t*. As such, ω_u is a fixed value and hence $\Delta\omega \to 0$ as $N \to \infty$ so that $N\,\Delta\omega = \omega_u$.

The non-stationary is then introduced by multiplying each of the stationary time histories with modulating functions $A_j(t)$; $j = 1,2,...,n$. In the next step, the response spectra of the simulated non-stationary time histories are calculated and matched with the prescribed response spectra. In case, the response spectra do not match at a chosen level of accuracy, the diagonal terms of the cross-spectral density matrix of the underlying stationary are updated as shown in Fig. 1.

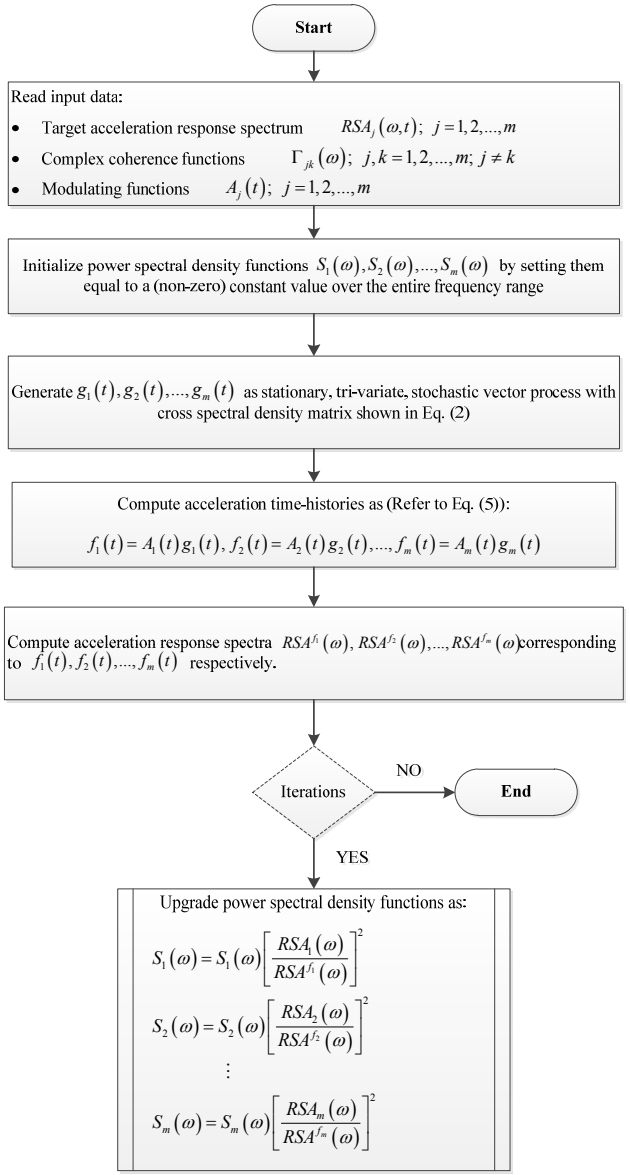

Figure 1. Simulation of seismic ground motions compatible with prescribed response spectra

3. NUMERICAL MODELING OF AN ARCH DAM

Double curvature Dez arch dam in Iran was selected as numerical example to investigate seismic behavior of the coupled system. Total height of Dez is 203m but the height of the main body (without concrete saddle) is 186m. Crest length is 240m and thickness at the crest level is 4.5m and its maximum thickness at the base is 21m. Generally, Dez categorized as asymmetry slender dam so its behavior must be studied precisely [20, 21].

3.1 FINITE ELEMENT MODEL

Finite element idealization prepared for the dam, foundation rock and reservoir is shown in Fig.2, which consists of 792 solid elements for modeling the dam body and concrete saddle, 3770 solid elements for simulation of mass-less foundation rock and 3660 fluid elements in reservoir domain. In this model, mostly hexagonal elements were used, while prism elements were utilized at portions of the model where geometry was not regular. Far-end boundary of the foundation is at the distance from the dam which is about 2 times the height of the dam body in all directions. The reservoir was modeled using hexagonal and prism fluid elements. Utilized Eulerian fluid elements have three translational degrees of freedoms (DOFs) and one pressure DOF in each node. It should be noted that translation DOFs are active only at nodes that are on the interface with solid elements [20]. The step-by-step methodology in order to solve the fluid-structure interaction problem was discussed by Mirzabozorg et al. [22]. In the present study, all contraction joints as well as peripheral joint were modeled using 3D node-to-node contact elements. These elements are only able to endure compression in normal direction to the joint surface and shear in tangential direction [21].

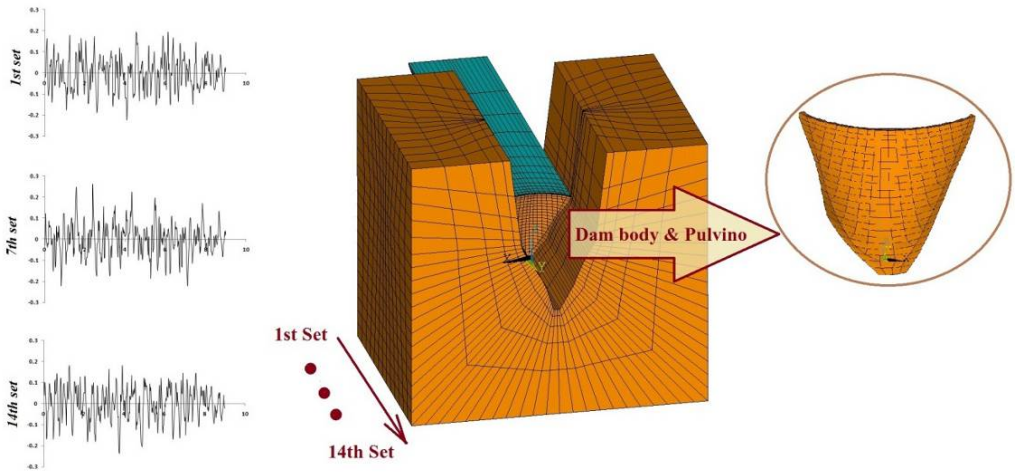

Figure 2. Finite element model of the coupled system and time-histories of ground motions at various locations on the foundation boundary

3.2 MATERIAL PROPERTIES

Material property of mass concrete and foundation rock are presented in table 1. In addition, reservoir water density is taken as 1000kg/m^3, sound velocity is 1440m/s in water and wave reflection coefficient for the reservoir around boundary is supposed 0.8, conservatively [20].

Table 1: Material property of mass concrete and foundation rock

	Properties	Static condition	Dynamic condition
Mass Concrete	Isotropic Elasticity	40GPa	46GPa
	Poisson's Ratio	0.2	0.14
	Mass Density	2400kg/m^3	2400kg/m^3
	Uniaxial Compressive Strength	$(f_c)_{static}$ = 35MPa	$(f_c)_{dynamic}$ =36.5MPa
	Uniaxial Tensile Strength	$(f_t)_{static}$ = 3.4MPa	$(f_t)_{dynamic}$ = 5.1MPa
Foundation Rock	Deformation Modulus (Saturated)	13GPa	13GPa
	Deformation Modulus (Unsaturated)	15GPa	15GPa
	Poisson's Ratio	0.25	0.25

4. LOADING THE SYSTEM

Applied loads on the system are dam body self-weight, hydrostatic pressure in Normal Water Level (NWL) and seismic load. In addition, thermal load corresponding to winter condition is applied on the dam body. The self weight was applied in such a way that the construction stages and joint grouting effects on the body response are taken into account. In addition, the reservoir impounding is gradual to simulate the real condition. It is worthy to note that thermal load applied on the structure has been extracted from calibrated thermal transient analyses conducted using real data at the dam site taking into account solar radiation on exposed surfaces of the dam body [20].

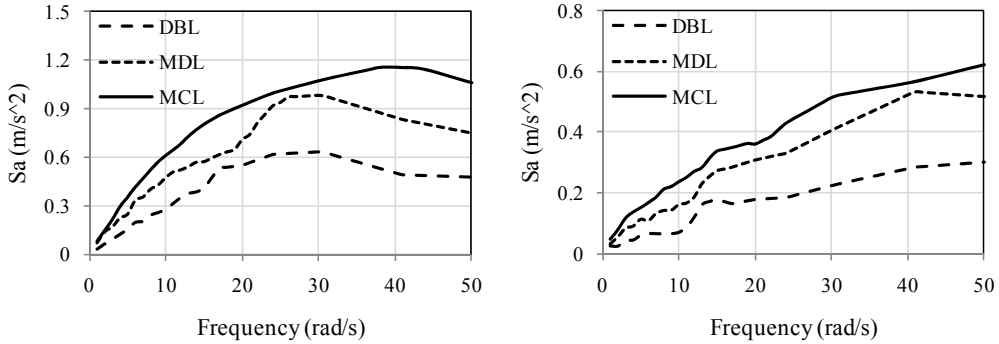

Figure 3. Acceleration response spectra for different performance levels; (a) Horizontal component;

(b) Vertical component.

To investigate the ground motions spatial variation effects on the response, three performance levels were selected which are design base level (DBL), maximum design level (MDL) and maximum credible level (MCL). Horizontal and vertical acceleration response spectrums of these levels extracted from hazard analysis of the dam site are shown in Fig. 3. Also time-history of horizontal and vertical component of the generated ground motions for uniform excitation are shown in Fig. 4. It is notable that in the case of uniform excitation exerted ground motion on all the supporting points are the same.

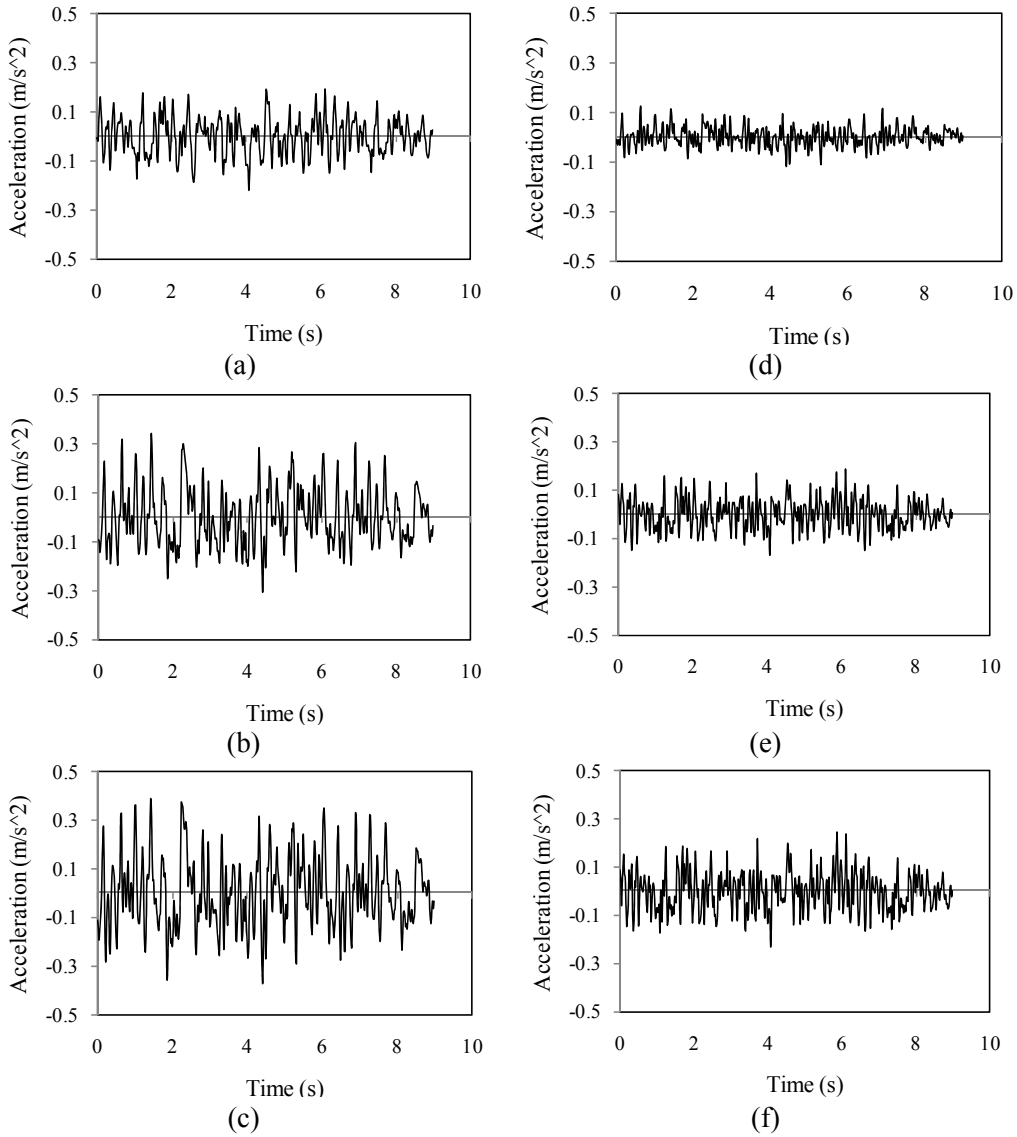

Figure 4. Acceleration time-histories in uniform excitation for various performance levels; (a) DBL-Horizontal component; (b) MDL- Horizontal component; (c) MCL- Horizontal component;

(d) DBL-Vertical component; (e) MDL-Vertical component; (f) MCL-Vertical component

For applying the non-uniform ground motions, the system is excited at foundation boundaries using 14 sets of simulated records (specified in upstream-downstream direction) compatible with desired spectrum as shown in Fig. 2. Based on the presented formulation in previous sections, a computer program was developed for generating non-uniform ground motions. The program is capable of producing different non-uniform acceleration time-histories considering wave-passage and incoherency effects according to the target spectrum. The wave passage velocity of the earthquake waves is taken as 2000m/s and the Newmark-β method is utilized to solve the coupled nonlinear problem of dam-reservoir-foundation model. Moreover, structural damping is taken to be 5% of critical damping in all cases.

5. RESULTS AND DISCUSSION

5.1 DISPLACEMENT

In this section, results of displacement at the crest obtained from uniform and non-uniform excitation analyses for the three performance levels are considered. As can be seen in Fig. 5, displacements in uniform and non-uniform excitations have more similarity in lower performance levels. In all cases seismic analyses are started after static and thermal analyses and the displacement time-histories are shifted to zero at the beginning of the seismic analyses due to the same values of the crest displacement at the end of the static stage. In DBL, general trend of two analyses are very close. In some parts uniform ground motion and in some others non-uniform ground motions lead to higher values in DS and US directions. In MDL two analyses show differences in all times. However, the peak values in DS direction are not so different. Finally, the displacement time histories corresponding to MCL leads to completely different time histories and the values corresponding to the analysis with multiple support excitations utilizing non-uniform ground motions increase during the time passage. Maximum displacement values for the mid-point, the right quarter and the left quarter points along the crest are summarized in table 2.

Table 2: Extreme values for displacement in stream direction along the crest

		Mid-point		**Right quarter point**		**Left quarter point**	
		US (mm)	**DS (mm)**	**US (mm)**	**DS (mm)**	**US (mm)**	**DS (mm)**
DBL	**Uniform**	55	31	22	17	20	14
	Non-uniform	45	23	27	24	140	0
MDL	**Uniform**	30	48	14	20	18	22
	Non-uniform	57	20	30	25	48	5
MCL	**Uniform**	40	70	20	30	18	24
	Non-	130	21	140	20	90	5

uniform

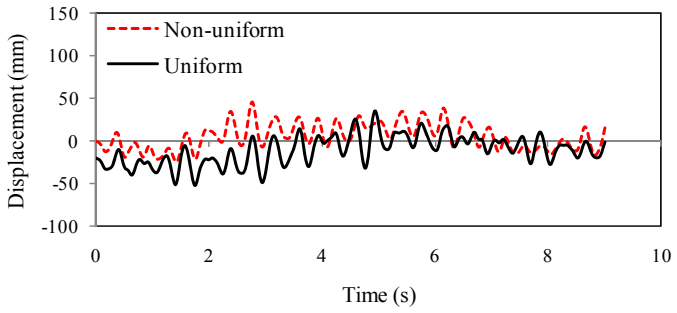

(a)

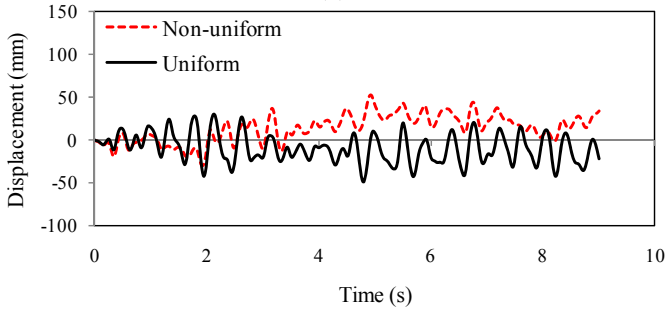

(b)

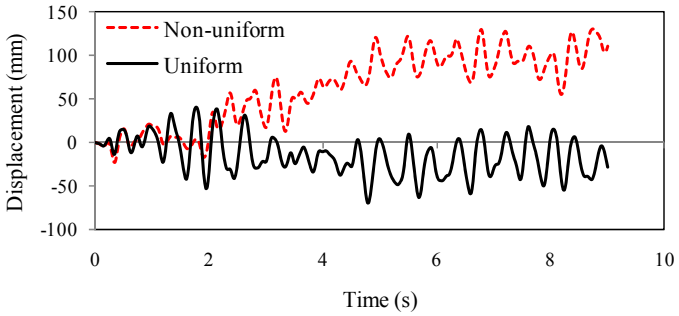

(c)

Figure 5. Displacement time-histories at the mid-point of the crest in stream direction; (a) DBL; (b) MDL; (c) MCL

5.2 PRINCIPAL STRESSES

Fig.6 shows time-histories of principal stresses at the crest on the central cantilever. As can be seen, multiple supports excitation leads to higher values for the first principal stress (S1) and lower values for the third principal stress (S3) and as expected, with increasing performance levels both principal stresses increase. Table 3 represents the extreme values occurred at the mid-point, right quarter and left quarter along the crest.As shown, S1at the central point of the crest extracted from multiple supports excitation is more than that obtained from uniform excitation but at the right quarter and left quarter points this is vice versa.

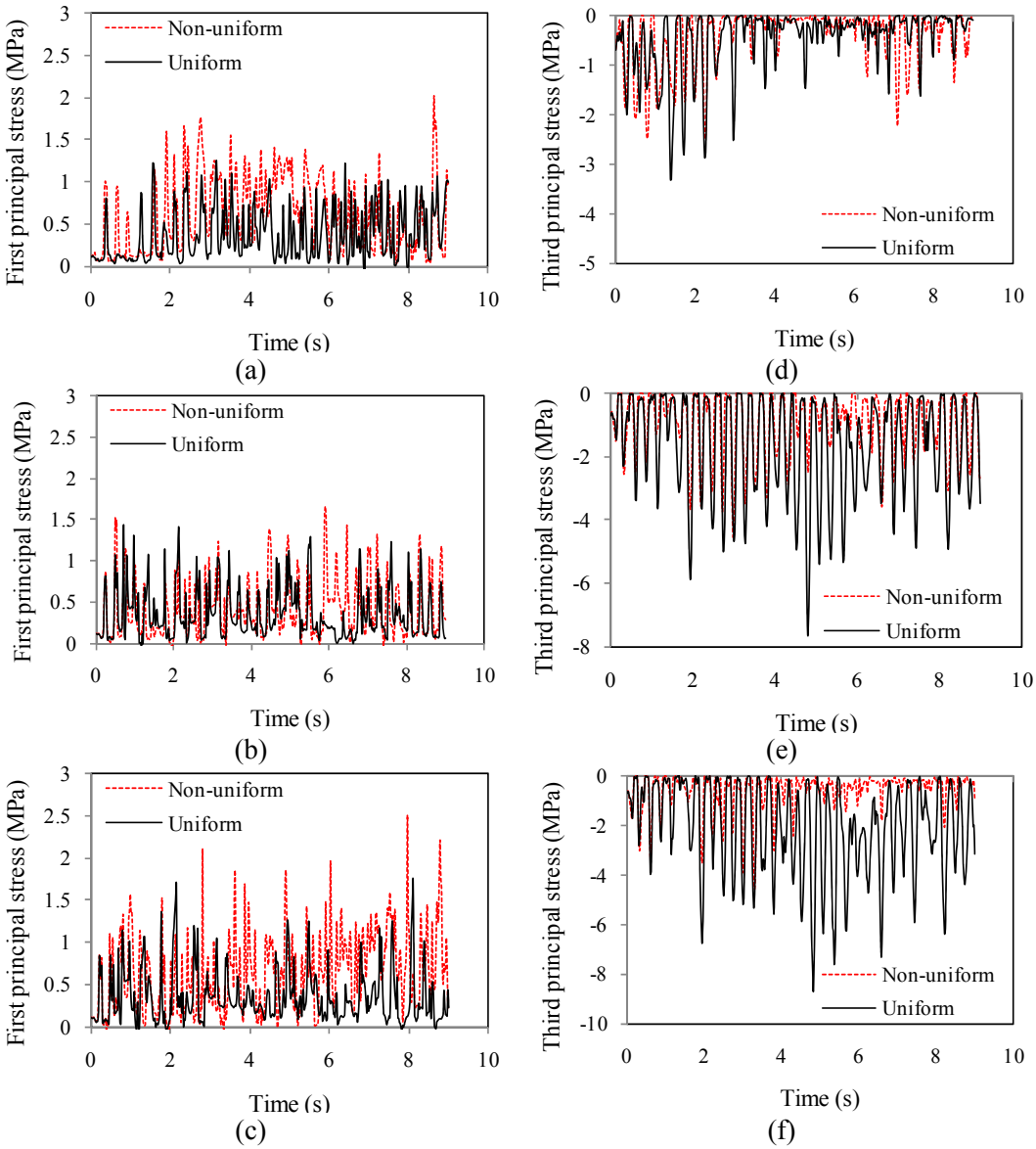

Figure 6. Principal stresses Time histories at mid-point of the crest; (a) DBL-S1; (b) MDL-S1; (c) MCL-S1; (d) DBL-S3; (e) MDL-S3; (f) MCL-S3

As shown in Fig. 6, increasing performance levels of earthquake leads to increasing the differences between the uniform and non-uniform excitation models. In addition, extreme values of S3at the mid-point, the right quarter and the left quarter points are shown in table 3.Generally, S3 at the mid-point of the crest extracted from uniform excitation analysis is more than that obtained from non-uniform excitation analysis. This phenomenon at the right quarter and the left quarter points is vice versa.

Table 3: Extreme values of principal stresses along the crest

		Mid-point		Right quarter point		Left quarter point	
		S1 (MPa)	**S3 (MPa)**	**S1 (MPa)**	**S3 (MPa)**	**S1 (MPa)**	**S3 (MPa)**
DBL	**Uniform**	1.20	-3.40	1.70	-5.80	1.00	-5.50
	Non-uniform	2.10	-2.60	1.30	-6.00	0.65	-5.50
MDL	**Uniform**	1.40	-8.00	1.60	-7.00	0.80	-7.50
	Non-uniform	1.70	-4.50	1.80	-6.80	0.60	-1.40
MCL	**Uniform**	1.75	-9.00	2.00	-7.00	1.00	-1.10
	Non-uniform	1.80	-4.50	1.80	-8.00	2.10	-8.00

5.3 JOINT OPENING AND SLIDING

Fig. 7 shows extreme values of joints opening/sliding experienced by the contact elements located on the upstream face along the crest. Obviously, increasing seismic performance level leads to higher joint opening and joint sliding. In DBL, joints sliding curves resulted from the two conducted analyses, i.e. uniform excitation and multiple supports exciting analyses are the same and joints opening curves have great consistency with each other. In MDL, although there is good consistency between the extracted results, there are some differences in joints opening at the central region and along the right portion of the crest especially in vicinity of the right abutment. However, the extreme values of the analysis with multiple supports exciting are lower. Finally, joints opening at the middle part and along the right side of the crest are completely different for the two conducted analyses at MCL. In addition, there is some difference in joints sliding along the right side of the crest.

Fig. 8 represents non-concurrent envelopes of joint opening/sliding along the height of the dam body experienced by the contact elements located between the central cantilever and the adjacent ones on the upstream face. As can be seen, for all the considered performance levels the uniform excitation leads to more regular curve in joint openings in comparison with those obtained from analyses with multiple supports excitation. In uniform exciting analyses, extreme openings occur at upper parts of the dam body in vicinity of the crest, while multiple supports excitation not only leads to higher values in joint openings but also changes general trend of the envelope and extreme values location. In the envelopes pertinent to the joint sliding, although some similarities are observed in ½ upper part of the dam body due to arch action and limiting the joint sliding, large differences are experienced in lower ½ part of the body. In DBL, non-uniform excitation leads to higher joint sliding for all contact elements along the dam height. In MDL and MCL, uniform excitation lead to higher sliding in lower parts and lower sliding in upper parts of the dam body. Generally, it can be concluded that along the crest points there is no considerable differences in extreme values of joints opening/sliding resulted from the two types of seismic excitations but

differences are meaningful along the upstream contact elements in central cantilever.

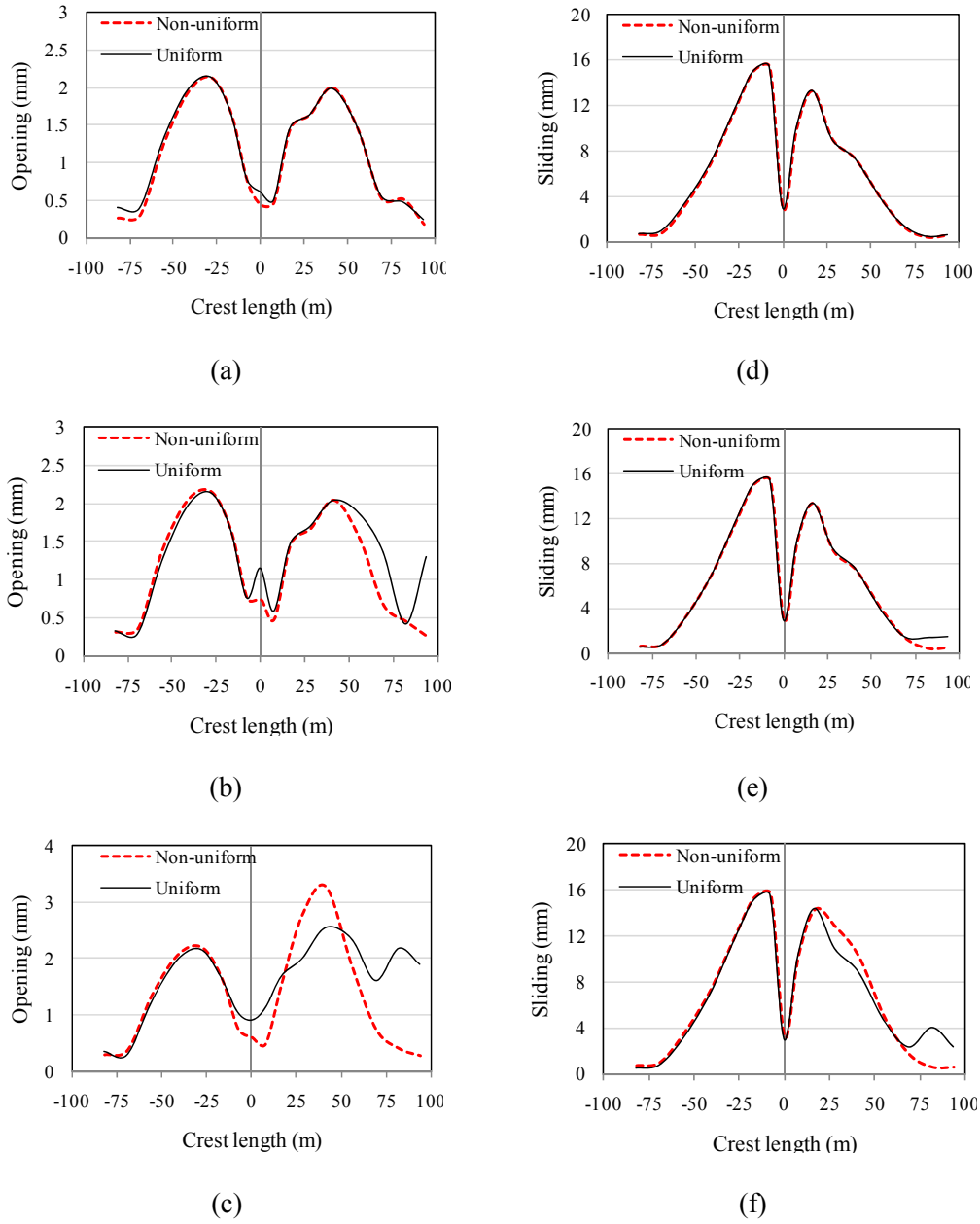

Figure 7. Extreme values for joints opening; (a) DBL; (b) MDL; (c) MCL and joints sliding; (d) DBL; (e) MDL; (f) MCL; experienced by upstream contact elements along the crest of the dam body

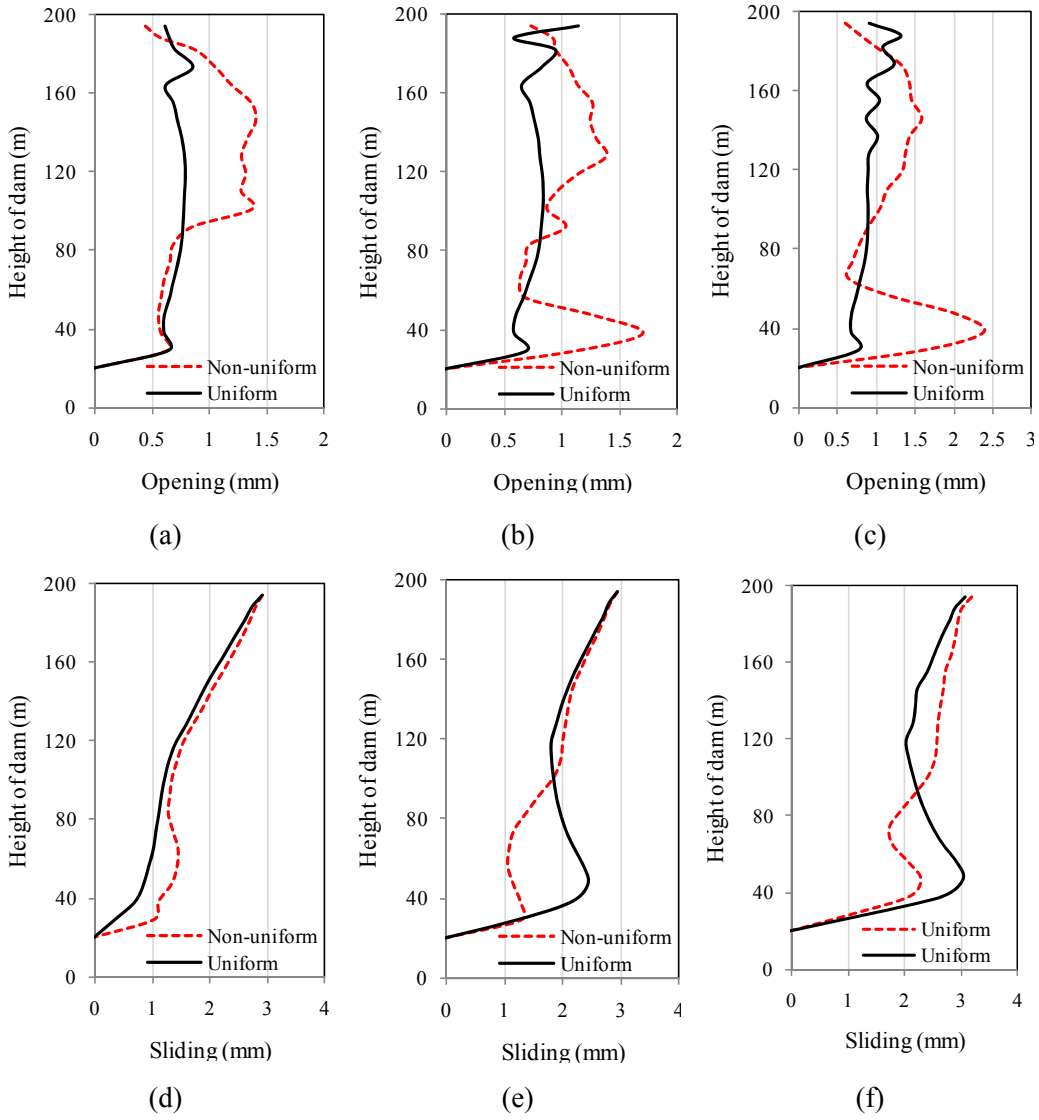

Figure 8. Extreme values for joint opening; (a) DBL; (b) MDL; (c) MCL; and for joint sliding; (d) DBL; (e) MDL; (f) MCL; experienced by upstream contact elements along the central block

5.4 Principal stresses

Figs. 9 and 10 represent non-concurrent envelopes of principal stresses extracted from uniform and non-uniform analyses on upstream and downstream faces of the dam body corresponding to DBL. As can be seen, in non-uniform excitation maximum value for tensile stress reaches to 9.69MPa which occurs at the lower part of the dam body in vicinity of the concrete saddle (called as Pulvino). In analysis with uniform excitation, the extreme values for S1occur on the upstream face at upper part of the dam body. The maximum value of the tensile stress in this analysis reaches to 3.85MPa. Neglecting local overstressed points

in non-uniform excitation (in vicinity of Pulvino), it can be seen that the areas with high stresses on the upstream face shift from left parts in the case with uniform excitation to lower parts in analysis with multiple supports excitation. In analysis with non-uniform excitation, the minimum value for S3 belongs to the central part on the upstream face and some areas on dam-Pulvino interface and its value reaches to -17.8MPa but in analysis with uniform excitation minimum value for S3 is -14.3MPa occurring at central part on the upstream face in vicinity of the crest.

The non-concurrent envelopes of principal stresses in MDL are depicted in Figs. 11 and 12. The overstressed areas for the first principal stress are concentrated in upper part on the downstream face in uniform excitation case while they shift to the lower parts on the upstream face and also some areas in vicinity of Pulvino in the case with non-uniform excitation. On the other hand, although general pattern of non-concurrent envelopes for the third principal stress on the upstream face are almost the same in the considered cases, multiple support exciting leads to concentration of high compressive stresses in lower parts on the downstream face.

In MCL (results are shown in Figs. 13 and 14), maximum first principal stress occurs in lower part of the dam for both considered cases. This value for the uniform and non-uniform excitation reaches to 4.5MPa and 12.48MPa, respectively. According to Fig. 14, the extreme value for the third principal stress occurs in lower part of the dam so that the extreme compressive stress corresponding to the case with uniform excitation is -18.5MPa and the corresponding one for the case with multiple support excitation reaches to -46.5MPa. It is noteworthy that the high values for the extreme values are limited to the local points.

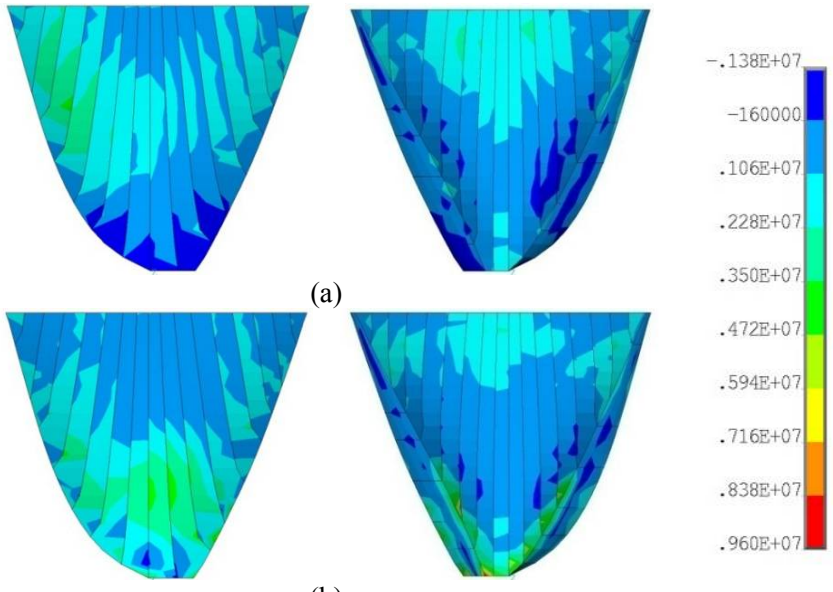

Figure 9. Non-concurrent envelope of the first principal stress on upstream and downstream faces for DBL (Pa); (a) Uniform excitation; (b) Non-uniform excitation

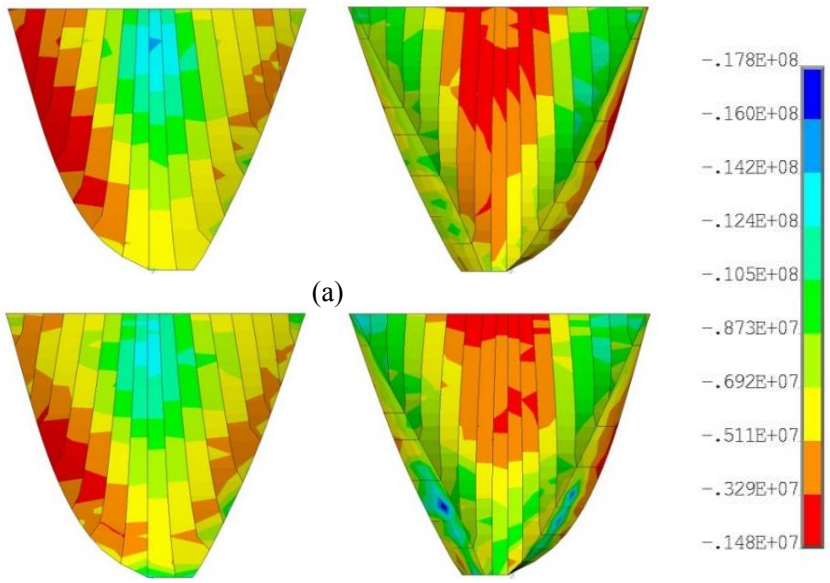

(a)

(b)

Figure 10. Non-concurrent envelope of the third principal stress on upstream and downstream faces for DBL (Pa); (a) Uniform excitation; (b) Non-uniform excitation

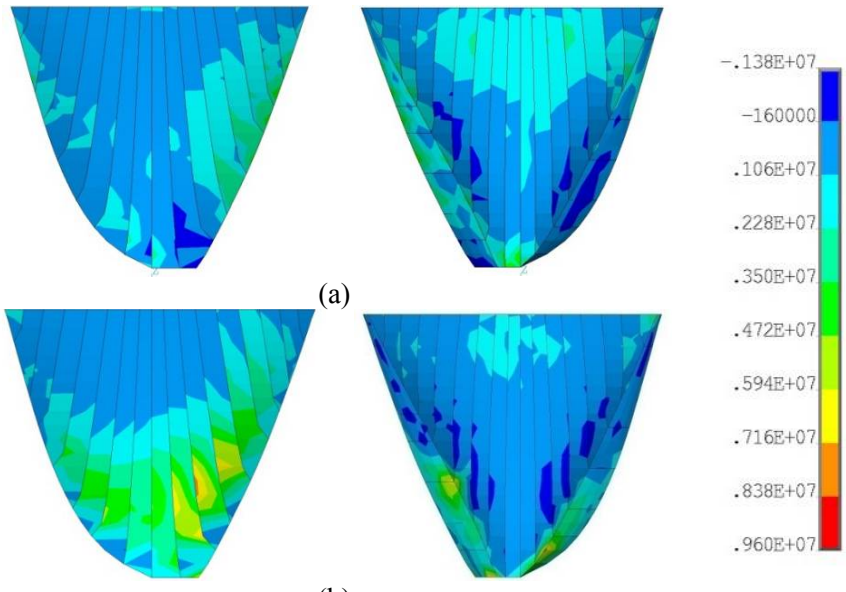

(a)

(b)

Figure 11. Non-concurrent envelope of the first principal stress on upstream and downstream faces for MDL (Pa); (a) Uniform excitation; (b) Non-uniform excitation

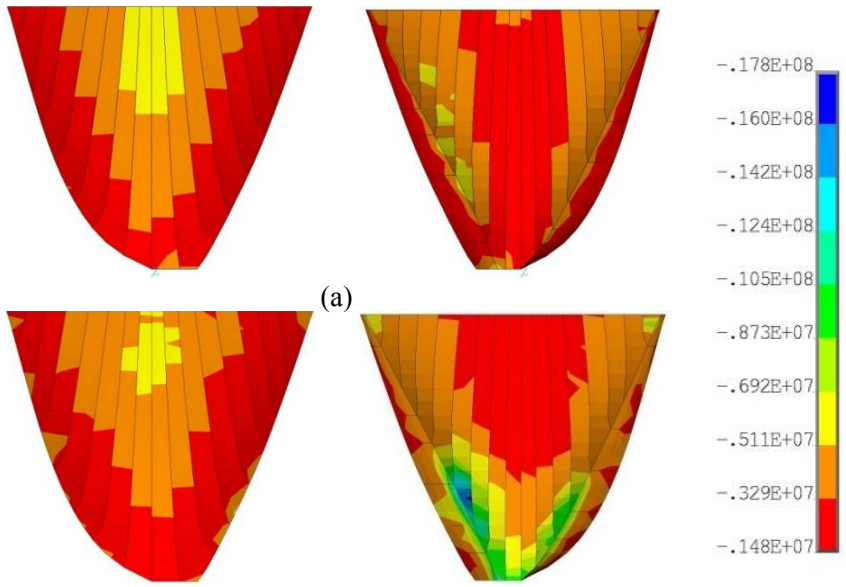

(a)

(b)

Figure 12. Non-concurrent envelope of the third principal stress on upstream and downstream faces for MDL (Pa); (a) Uniform excitation; (b) Non-uniform excitation

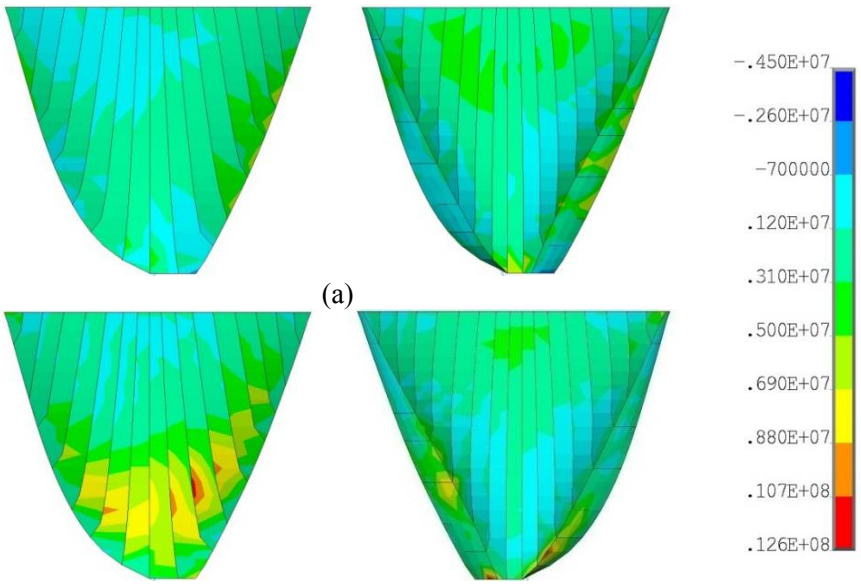

(a)

(b)

Figure 13. Non-concurrent envelope of the first principal stress on upstream and downstream for MCL (Pa); (a) Uniform excitation; (b) Non-uniform excitation

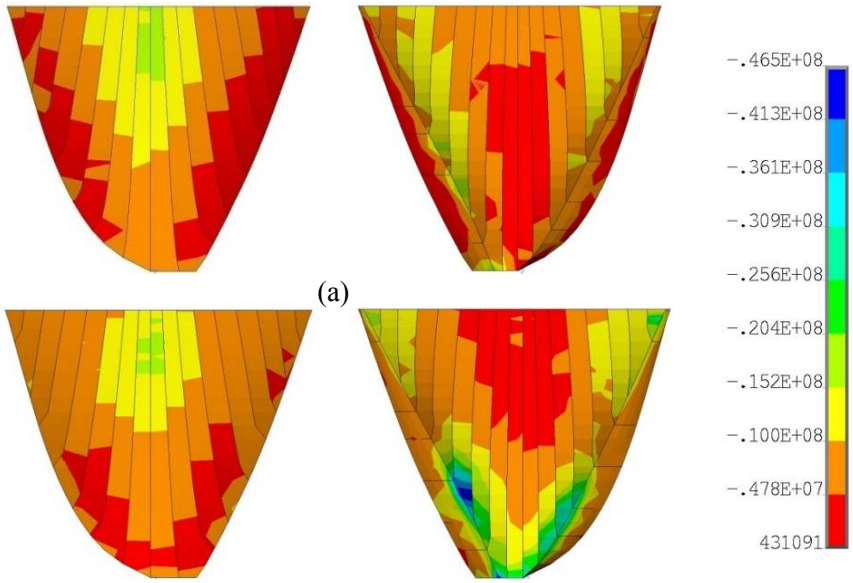

(a)

(b)

Figure 14. Non-concurrent envelope of the third principal stress on upstream and downstream faces for MCL (Pa); (a) Uniform excitation; (b) Non-uniform excitation

6. CONCLUSION

In this paper, effects of non-uniform excitation due to spatially varying ground motions on nonlinear responses of concrete arch dams in three seismic performance levels were considered.A double curvature arch dam was selected as numerical example to investigate seismic behavior of the coupled system. Reservoir was modeled as compressible material and foundation was supposed as mass-less medium. In addition, all contraction joints and also, peripheral joint between the main body and its Pulvino were modeled as recorded in as-built drawings. A code was developed for generating non-uniform ground motions due to wave passage and incoherency in which Monte Carlo simulation approach was utilized. The generated ground motions are compatible with the target response spectra. Several analyses with various characteristics were conducted. It was concluded that displacements in uniform and non-uniform excitations are comparable with each other in DBL and MDL, whileuniform excitation causes larger displacement than non-uniform excitation. In MCL, large differences are observed between results obtained from the cases with uniform and non-uniform excitation. Usually, displacement at mid-point of the crest in uniform excitation is more than that obtained applying non-uniform excitation but at the right quarter and left quarter points, this is contrary.

Along the crest, it was found that joints opening at the middle part and along the right side are completely different for the two conducted analyses at MCL. In addition, there is some difference in joints sliding along the right side of the crest in this level of excitation. However, these differences are less in DBL and MDL. Generally, it was concluded that

there is no notable differences in extreme values of joints opening/sliding resulted from the two types of seismic excitations along the crest. However, the differences are meaningful for the upstream contact elements along the height of the body in central cantilever.

Applying non-uniform excitation leads to higher values for the first principal stress (S1) and lower values for the third principal stress (S3) at mid-point of the crest but at the right quarter and left quarter points along the crest, the behaviour is contrary. As expected, with increasing levels of earthquake, the extreme values increase and differences between obtained results applying uniform and non-uniform excitations increase.In addition, it is concluded that differences between results for the first principal stress is more than for the third principal stress. About principal stress distribution within the body, it was found that neglecting overstressed local points, the areas with high stresses on the upstream face shifted from left parts in uniform excitation to lower parts in non-uniform excitation.Comparing the results in three seismic hazard levels, it was found that the extreme values for the stresses in the cases with non-uniform excitation is more than those obtained applying uniform excitation and effect of multi-support excitation on the first principal stress is more intensive.

It is generally observed that the spatially varying earthquake ground motion causes significant changes on the structural responses of the dam-reservoir-foundation system. Therefore, spatially varying earthquake ground motions should be incorporated in seismic safety evaluation and seismic design of large dams.

REFERENCES

1. Zerva A, Zervas V. Spatial variation of seismic ground motions: An overview, *Applied Mechanics Reviews*. No. 3, **55**(2002) 271-97.
2. Der Kiureghian A. A coherency model for spatially varying ground motions, *Earthquake Engineering & Structural Dynamics*, **25**(1996), 99-111.
3. Chen MT, Harichandran RS. Response of an earth dam to spatially varying earthquake ground motion, *Journal of Engineering Mechanics*, N0.9, **127**(2001) 932-9.
4. Bayraktar A, Dummsnoglu AA. The effect of synchronous ground motion on hydrodynamic pressures, *Computer & Structures*, **68**(1998) 271-82.
5. Bayraktar A, Dummsnoglu AA, Calayir Y. Asynchronous dynamic analysis of dam-reservoir-foundation systems by the Lagrangian approach, *Computer & Structures*, **58**(1996) 925-35.
6. Maeso O, Aznarez JJ, Dominguez J. Effects of space distribution of excitation on seismic response of arch dams, *Journal of Engineering Mechanics*, **128**(2002) 759-68.
7. Nowak PS, Hall JF. Arch dam response to nonuniform seismic input, *Journal of Engineering Mechanics*, **116**(1990) 125-39.
8. Alves SW, Hall JF. Generations of spatially nonuniform ground motion for nonlinear analysis of a concrete arch dam, *Earthquake Engineering & Structural Dynamics,* **35**(2006) 1339-57.
9. Alves SW, Hall JF. System identification of a concrete arch dam and calibration of its finite element model, *Earthquake Engineering and Structural Dynamics*, **35**(2006) 1321-

37.
10. Bayraktar A, Hancera E, Dumanoglu AA. Comparison of stochastic and deterministic dynamic responses of gravity dam-reservoir systems using fluid finite elements, *Finite Elements in Analysis and Design*, **41**(2005) 1365-76.
11. Mirzabozorg H, Varmazyari M, Ghaemian M. Dam- reservoir-massed foundation system and travelling wave along reservoir bottom, *Soil Dynamics and Earthquake Engineering*, **30**(2010) 746-56.
12. Haciefendioğlu K, Soyluk K. Nonlinear Response of Earth fill Dams to Spatially Varying Ground Motion Including Site Response Effect, *Advances in Structural Engineering*. No.2, **14**(2011) 223-34.
13. Chopra A, Wang J. Earthquake response of arch dams to spatially varying ground motion, *Earthquake Engineering and Structural Dynamics*, No.8, **39**(2010) 887-906.
14. Wang J, Chopra A. Linear analysis of concrete arch dams including dam water foundation rock interaction considering spatially varying ground motions, *Earthquake Engineering and Structural Dynamics*, No.7, **39**(2010) 731-50.
15. Mirzabozorg H, Akbari M, Hariri-Ardebili MA. Wave Passage and Incoherency Effects on Seismic Response of High Arch Dams, *Earthquake Engineering and Engineering Vibration*, No.4, **11**(2012) 567-578.
16. Deodatis G. Non-stationary stochastic vector processes: Seismic ground motion applications. *Probabilistic Engineering Mechanics*, **11**(1996) 149-67.
17. Saxena V. *Spatial Variation of Earthquake Ground Motion and Development of Bridge Fragility Curves*, Ph.D. Dissertation, Department of Civil and Environmental Engineering, Princeton University, Princeton, NJ, USA, 2000.
18. Shinozuka M, Deodatis G. Stochastic process models of earthquake ground motion, *Journal of Probabilistic Engineering Mechanics*, No.3, **3**(1988) 114-23.
19. Kim S, Feng MQ. Fragility analysis of bridges under ground motion with spatial variation. *International Journal of Non-Linear Mechanics*, No.5, **38**(2003) 705-21.
20. Hariri-Ardebili MA, Mirzabozorg M, Ghaemian M, Akhavan A, Amini A. Calibration of 3D FE model of DEZ high arch dam in thermal and static conditions using instruments and site observation, *6th International Conference on Dam Engineering*, Lisbon, Portugal, (2011) 121-135.
21. Hariri-Ardebili MA, Mirzabozorg H, Seismic Performance Evaluation and Analysis of Major Arch Dams Considering Material and Joint Nonlinearity Effects, *ISRN Civil Engineering*, **2012**(2012), Article ID 681350, 10 pg.
22. Mirzabozorg H, Hariri-Ardebili MA, Nateghi-A R. Free Surface Sloshing Effect on Dynamic Response of Rectangular Storage Tanks, *American Journal of Fluid Dynamics*, No.4, **2**(2012) 23-30.